Geochemical Perspectives Letters

The end of the isotopic evolution of atmospheric xenon

L. Ardoin[1,2*], M.W. Broadley[1], M. Almayrac[1], G. Avice[3], D.J. Byrne[1], A. Tarantola[4], A. Lepland[5], T. Saito[6], T. Komiya[7], T. Shibuya[6], B. Marty[1]

https://doi.org/10.7185/geochemlet.2207

Abstract

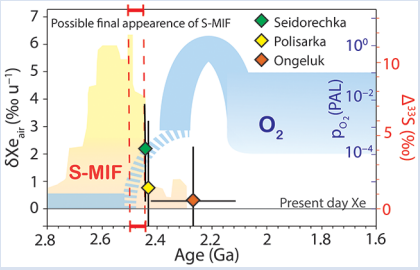

Noble gases are chemically inert and, as such, act as unique tracers of physical processes over geological timescales. The isotopic composition of atmospheric xenon, the heaviest stable noble gas, evolved following mass-dependent fractionation throughout the Hadean and Archaean aeons. This evolution appears to have ceased between 2.5 and 2.1 Ga, around the time of the Great Oxidation Event (GOE). The coincidental halting of atmospheric Xe evolution may provide further insights into the mechanisms affecting the atmosphere at the Archaean-Proterozoic transition. Here, we investigate the isotopic composition of Xe trapped in hydrothermal quartz from three formations around the GOE time period: Seidorechka and Polisarka (Imandra-Varzuga Greenstone Belt, Kola Craton, Russia) with ages of 2441 ± 1.6 Ma and 2434 ± 6.6 Ma, respectively, and Ongeluk (Kaapvaal Craton, South Africa) dated at 2114 ± 312 Ma (Ar-Ar age) with a host formation age of 2425.6 ± 2.6 Ma (upper bound). From these analyses we show that Xe isotope fractionation appears to have ceased during the time window delimited by the ages of the Seidorechka and Polisarka Formations, which is concomitant with the disappearance of mass-independent fractionation of sulfur isotopes (MIF-S) in the Kola Craton. The disappearance of Xe isotope fractionation in the geological record may be related to the rise in atmospheric oxygen and, thus, can provide new insights into the triggering mechanisms and timing of the GOE.

Received 29 October 2021 | Accepted 1 February 2022 | Published 10 March 2022

Introduction

Due to their chemical inertness, noble gases (He, Ne, Ar, Kr, Xe) constitute powerful geochemical tracers for constraining physical processes occurring in the Earth's atmosphere. Atmospheric xenon is of particular interest because its isotopic composition is highly mass-dependently fractionated (MDF) by 41.5 ‰ u^{-1} when compared to its presumed primitive ancestor U-Xe (Pepin, 1991). Studies of palaeo-atmospheric Xe trapped in Archaean rocks (mainly as fluid inclusions in hydrothermal quartz) have shown that the evolution of isotopic fractionation of Xe was a long-term process that took place during the Hadean and the Archaean aeons. This protracted MDF appears to be unique to Xe, with no evidence that the other noble gases underwent progressive fractionation (Pujol *et al.*, 2011; Avice *et al.*, 2018; Almayrac *et al.*, 2021). Such Xe specific evolution has been attributed to preferential, non-thermal escape of xenon from the Earth's atmosphere to space upon ionisation by solar UV photons (Pujol *et al.*, 2011; Hébrard and Marty, 2014; Avice *et al.*, 2018) and subsequent entrainment by escaping hydrogen ions (Zahnle *et al.*, 2019). Available data indicate that the evolution of the isotopic composition of atmospheric xenon ceased at some point between 2.6 and 1.8 Ga (Avice *et al.*, 2018).

Xenon is the second atmospheric element for which a stable isotope fractionation during the Archaean aeon has been observed, with the mass-independent fractionation of sulfur isotopes (MIF-S) being characteristic for Archaean age samples (Farquhar and Wing, 2003; Philippot *et al.*, 2018). The MIF-S signature was likely produced by interactions between volcanic sulfur species and ultraviolet radiation, and shows a sharp transition and collapse during the Great Oxidation Event (GOE) (Farquhar and Wing, 2003). Conversely, the Xe isotope evolution was a gradual and cumulative process, causing atmospheric Xe to become increasingly fractionated with time. Furthermore, the GOE is understood to have stopped the generation of MIF-S, as ozone from free oxygen in the atmosphere shielded solar UV photons. For Xe, it is not clear if the GOE was also responsible for stopping Xe^+ escape, and which environmental parameters (*e.g.*, atmospheric composition, hydrogen escape, solar activity) may have changed to prevent Xe from escaping the Earth's atmosphere.

1. Université de Lorraine, CNRS, CRPG, F-54000 Nancy, France
2. Now at: Université Libre de Bruxelles CP160/03 Av. F.D. Roosevelt 50, 1050 Brussels, Belgium
3. Université de Paris, Institut de physique du globe de Paris, CNRS, F-75005 Paris, France
4. Université de Lorraine, CNRS, GeoRessources laboratory, BP 70239, F-54506, Vandœuvre-lès-Nancy, France
5. Geological Survey of Norway, 7491 Trondheim, Norway
6. Institute for Extra-cutting-edge Science and Technology Avant-garde Research (X-star), Japan Agency for Marine-Earth Science and Technology (JAMSTEC), 2-15, Natsushima-cho, Yokosuka 237-0061, Japan
7. Department of Earth Science and Astronomy, University of Tokyo, Tokyo, Meguro, 153-8902, Japan

* Corresponding author (email: lisa.ardoin@ulb.be)

In order to investigate the end of atmospheric MDF-Xe and to assess if it was coincidental with the GOE, we have analysed noble gases extracted from fluid inclusions from well-characterised hydrothermal quartz with ages encompassing that of the GOE. Using a new cumulative crushing technique, adapted from the procedure first used by Péron and Moreira (2018), allows the extraction of gas from much larger sample quantities, resulting in smaller analytical uncertainties (Supplementary Information). This is required to detect the low levels of Xe fractionation relative to the modern atmosphere that are observed close to the GOE. The samples measured in this study are, from oldest to youngest, Seidorechka (FD1A) and Polisarka (FD3A) Sedimentary Formations (Imandra-Varzuga Greenstone Belt, Kola Craton, Russia), and from the Ongeluk Formation (Kaapvaal Craton, South Africa). Depositional ages of FD1A and FD3A have been constrained between 2501.5 ± 1.7 Ma and 2441 ± 1.6 Ma (Amelin *et al.*, 1995), and 2441 ± 1.6 Ma and 2434 ± 6.6 Ma (Brasier *et al.*, 2013), respectively. The lower bounds of these time intervals are defined by the ages of overlying volcanic formations that are considered contemporaneous with quartz veining in underlying sediments. The Ongeluk Formation has been dated at 2114 ± 312 Ma (Ar-Ar age; Saito *et al.*, 2018) with an upper bound defined by the host formation age of 2425.6 ± 2.6 Ma (Gumsley *et al.*, 2017).

Preservation of Ancient Atmospheric Xe

Fluid inclusions can potentially preserve the noble gas signature of the ancient atmosphere (Pujol *et al.*, 2011). The petrographical study of the inclusions of the Ongeluk Formation performed by Saito *et al.* (2018) and our study of samples from the Kola Craton (FD1A and FD3A) indicate that a majority of the fluid inclusions have been trapped during quartz growth (Supplementary Information). The Ar and Xe content of the quartz fluid inclusions were measured using a Thermofisher Helix MC Plus© mass spectrometer at CRPG. The new extraction method was performed on FD1A and FD3A and consists of accumulating the extracted gases after crushing steps in an empty and previously evacuated steel bottle (Péron and Moreira, 2018; Péron *et al.*, 2021).

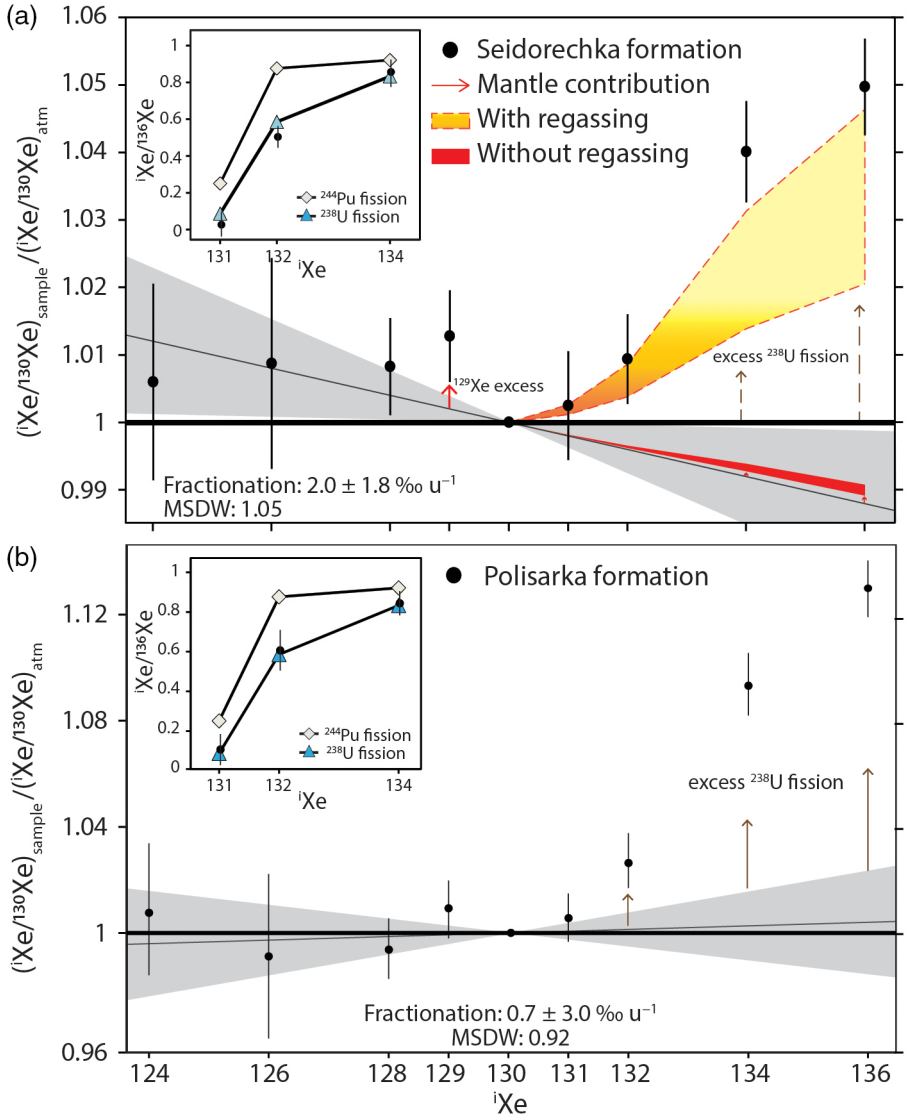

Figure 1 Isotopic spectrum of Xe released from fluid inclusions in **(a)** sample FD1A and **(b)** sample FD3A. The grey line and its associated envelope (2σ) correspond to the isotopic trend of the ^{124,126,128,130}Xe. **(a)** Mantle excesses of ^{131,132,134,136}Xe are estimated using the ^{129}Xe excess (Supplementary Information). Individual error bars are at 2σ.

Table 1 Isotopic ratio of the noble gases released by crushing and Xe fractionation. The fractionation was calculated from the $^{124,126,128}Xe/^{130}Xe$ ratios. The ratios are the weighted average of several replicates (Table S-3).

Samples	^{124}Xe	^{126}Xe	^{128}Xe	^{129}Xe	^{131}Xe	^{132}Xe	^{134}Xe	^{136}Xe	$^{40}Ar/^{36}Ar$	Xe Fractionation (‰ u^{-1})
	$^{130}Xe = 1$									
Air Ozima and Podosek (2002)	0.0234	0.0218	0.4715	6.496	5.213	6.607	2.563	2.176	298	
Ongeluk fm	0.0233	0.0220	0.4707	6.540	5.188	6.632	2.603	2.229	4570	**−0.3**
errors (2σ)	±0.0005	±0.0004	±0.0040	±0.066	±0.050	±0.640	±0.220	±0.020	±1488	±2.4
FD1A	0.0235	0.0220	0.4745	6.578	5.235	6.669	2.666	2.284	3010	**−2.0**
errors (2σ)	±0.0004	±0.0004	±0.0034	±0.026	±0.068	±0.044	±0.0192	±0.016	±504	±1.8
FD3A	0.0235	0.0216	0.4684	6.554	5.243	6.778	2.801	2.458	3639	**0.7**
errors (2σ)	±0.0006	±0.0006	±0.0054	±0.056	±0.044	±0.056	±0.028	±0.024	±610	±3.0

All our analyses present an excess of ^{40}Ar relative to modern atmospheric Ar with a minimum $^{40}Ar/^{36}Ar$ ratio of 1760 ± 18, from one crush of the Ongeluk Formation (Table S-4), attesting to limited exchange, if any, with modern atmospheric Ar. The $^{131,132,134,136}Xe$ excesses detected for all our samples correspond to a contribution from the spontaneous fission of ^{238}U (Fig. 1). We computed linear regressions on $^{124,126,128}Xe/^{130}Xe$ isotope ratios using the IsoplotR software (Vermeesch, 2018). The oldest sample, FD1A, presents a fractionation of 2.0 ± 1.8 ‰ u^{-1} (2σ; Fig. 1a) compared to the present day atmosphere. The FD3A (0.7 ± 3.3 ‰ u^{-1}, Fig. 1b) and Ongeluk quartz (–0.3 ± 2.4 ‰ u^{-1}, Fig. S-2), the youngest samples, do not display a resolvable MDF-Xe signature beyond uncertainty at 2σ (Table 1). Compared to modern atmospheric Xe ($^{129}Xe/^{130}Xe = 6.50$; Ozima and Podosek, 2002), the samples preserve small excesses of radiogenic ^{129}Xe ($^{129}Xe/^{130}Xe$ of 6.58 ± 0.04, 6.55 ± 0.06 and 6.54 ± 0.07 for FD1A, FD3A and Ongeluk Formation samples, respectively). It is the opposite of what is usually observed in samples from the Archaean aeon (Avice *et al.*, 2017; Bekaert *et al.*, 2018). The mono-isotopic depletion in ^{129}Xe within the Archaean atmosphere is thought to have been compensated by the progressive release of ^{129}Xe from the mantle throughout the Archaean aeon (Marty *et al.*, 2019). The ^{129}Xe excess in the oldest sample, FD1A, is therefore likely to be due to a local input of mantle-derived Xe in the hydrothermal fluids from which the quartz precipitated. A mantle Xe input could potentially account for the light Xe isotope excesses measured in the samples, especially when considering Xe in the Archaean mantle was likely primordial (chondritic; Broadley *et al.*, 2020). We ruled out this possibility because the $^{128}Xe/^{130}Xe$ of FD1A is inconsistent with mixing between the primordial mantle and modern atmosphere (Fig. S-4), and atmospheric regassing of the mantle was likely to be inefficient during the Archaean aeon (Péron and Moreira, 2018). Mantle contributions are then negligible (Table S-1; Supplementary Information) and excesses of $^{124,126,128}Xe$ in FD1A are considered to reflect the ancient atmospheric composition.

Link between Xe Fractionation and MIF-S

From our analyses we have shown, for the first time, that MDF-Xe signals disappear between two well-characterised Kola Craton sedimentary formations, implying that the fractionation process stopped between 2441 ± 1.6 Ma and 2434 ± 6.6 Ma (Fig. 2). Previous data from Avice *et al.* (2018) indicated that MDF-Xe was observable throughout the Archaean and into the Palaeoproterozoic era until 2 Ga. The difference between these previous data and our new results can be explained by (i) the age of the fluid inclusions containing the atmospheric Xe, and (ii) the precision required to distinguish between the present day atmosphere and the small extent of isotope fractionation of Xe present in fluid inclusion formed close to the cessation of Xe evolution. The fluid inclusion inventory reflects the atmospheric composition at the last equilibration with the atmosphere, which may be different from the age of quartz precipitation. Thus, the 6.5 ± 1.5 ‰ u^{-1} recorded in the 3.7 Ga Isua rocks that was attributed to a resetting metamorphic event at 2.3 Ga (Avice *et al.*, 2018) may, in fact, reflect an older atmospheric composition. Because the gas accumulation method is more precise than those used previously (Avice *et al.*, 2018), we could identify a slight MDF-Xe for sample FD1A at the 2σ precision level. Considering the 2σ error range for the fractionation of Xe in previously studied 2.1 ± 0.1 Ga Gaoua (Burkina Faso) and the 2.0 ± 0.1 Ga Carnaiba (Brazil) samples gives values of 2.6 ± 4.2 and 1.8 ± 4.4 ‰ u^{-1} for the fractionation of atmospheric Xe (Avice *et al.*, 2018). These values are both within uncertainty of modern atmosphere, and therefore it is not clear whether they, in fact, contained a fractionated atmospheric Xe signature.

The MDF-Xe evolution results from a poorly understood cumulative process, which took place during the Hadean and Archaean periods. Storage of Xe^+ into an organic haze and the contemporary loss of the residual Xe from space could explain the observed fractionation (Hébrard and Marty, 2014). This process would stop in an O_2-rich atmosphere that would halt the production of the haze. However, this possibility would still necessitate the escape of non-trapped Xe and therefore an additional, not yet identified, process is required. The escape of hydrogen ions to space entraining Xe^+ has been also previously suggested to account for both the oxidation of the atmosphere and the unique fractionation of Xe isotopes (Zahnle *et al.*, 2019). Consequently, this model leads to the oxidation of the surface reservoirs, including the crust, to the point where O_2 became stable enough to compete with atmospheric reduced gases, such as H_2 and CH_4 (Zahnle *et al.*, 2019). According to our data, the MDF-Xe signal disappears and the present day composition is reached between ~2441 and ~2434 Ma (Fig. 2). Sustaining a continuous escape of ionised hydrogen from the Earth formation until the GOE depends on many parameters including the strength of the Earth's magnetic field, the level of solar extreme ultraviolet (EUV) irradiation and the amount of hydrogen present in the atmosphere (Zahnle *et al.*, 2019). In the case of discrete escape episodes rather than a constant rate of atmospheric Xe-loss, our results imply a final burst occurring simultaneously with the initiation of the GOE.

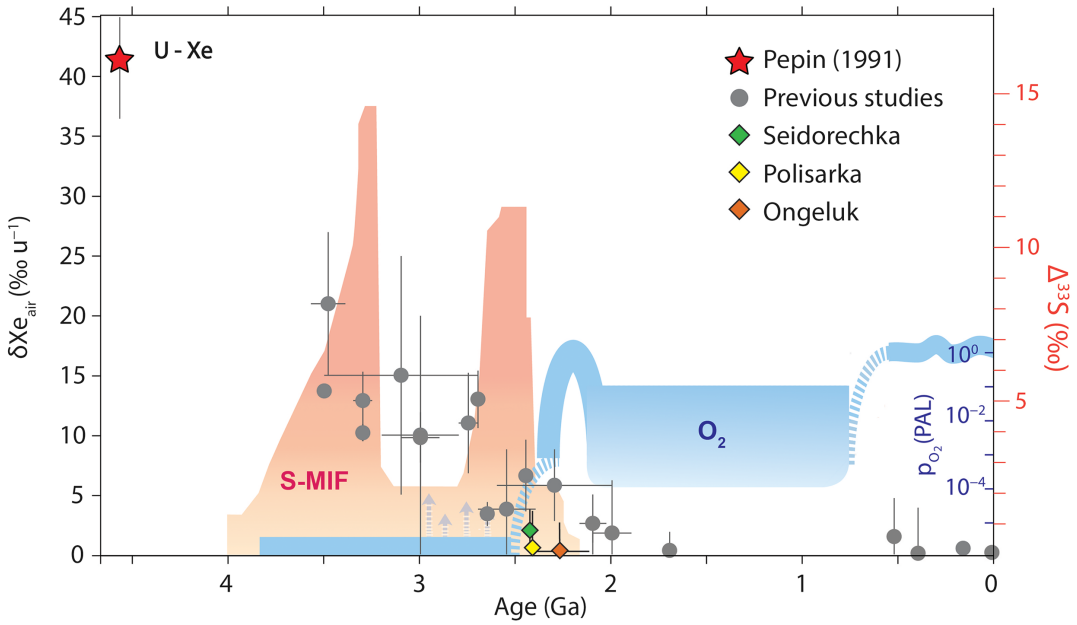

Figure 2 Records of atmospheric oxygen (O_2, blue; Lyons *et al.*, 2014), mass-independent fractionation of sulfur isotopes (MIF-S, orange; data from Killingsworth *et al.*, 2019) and mass dependent fractionation of xenon isotopes throughout Earth's history (Pepin, 1991; Avice *et al.*, 2018; Almayrac *et al.*, 2021), uncertainties are at 2σ.

The end of MDF-Xe between FD1A and FD3A is coincident with the disappearance of MIF-S as recorded in the sedimentary rocks hosting the quartz veins (Warke *et al.*, 2020). Sulfur isotopes represent an instantaneous record of the oxidation states of the atmosphere, at a local scale. MDF-Xe is the result of a cumulative process at global scale so it is likely that these geochemical markers would not be exactly simultaneous in their cessation. In light of the S-Xe relationship, it appears that the atmospheric process traced by Xe isotopes is linked with the oxidation state of the terrestrial atmosphere (Avice *et al.*, 2018).

The formation of the ozone layer as a consequence of O_2 rise in the atmosphere accounts for the end of the MIF-S signature (Farquhar and Wing, 2003; Lyons *et al.*, 2014). However, MIF-S signals could be preserved under oxidative weathering and then obscure the MIF/MDF transition due to a memory effect (Philippot *et al.*, 2018). This leads to a delay between the rise of oxygen and the disappearance of MIF-S signals of about 2.32 Ga (Gumsley *et al.*, 2017; Poulton *et al.*, 2021). Moreover, some environments may require more time to adapt and become permanently oxygenated after the end of hydrogen escape (Lyons *et al.*, 2014). Contrary to the MIF-S, hydrodynamic escape is not affected by the ozone formation (Zahnle *et al.*, 2019), and may be more sensitive to O_2 availability. Thus, the end of MDF-Xe fractionation could mark the time when atmospheric escape of hydrogen ceased, and ceased to contribute to the change of the redox ratio of Earth's surface reservoirs. It is important to underline the fact that Xe fractionation is a cumulative process: local variation of the signal cannot occur, unlike sulfur (Philippot *et al.*, 2018). In light of this, Xe is a reliable tracer and may better constrain the rise of oxygen levels within the atmosphere.

Conclusion

We have measured an isotopically fractionated Xe composition of 2.0 ± 1.8 ‰ u^{-1} relative to modern atmosphere at 2441 ± 1.6 Ma. A slightly younger sample of 2434 ± 6.6 Ma does not record any such fractionation, and is indistinguishable from the modern atmospheric composition. The disappearance of isotopically fractionated Xe signals could be a consequence of O_2 accumulation in the atmosphere. A temporal link between the disappearance of the Xe isotopes fractionation and the MIF-S signature at the Archaean-Proterozoic transition is clearly established for the Kola Craton. The mass-dependent evolution of Xe isotopes is the indication of a cumulative atmospheric process that may have played an important role in the oxidation of the Earth's surface (Zahnle *et al.*, 2019), independently of biogenic O_2 production that started long before the permanent rise of O_2 in the atmosphere (Lyons *et al.*, 2014).

Acknowledgements

This study was supported by the European Research Council (ERC) under the European Union's Horizon 2020 research and innovation programme (PHOTONIS Advanced Grant # 695618). We thank the Super-Cutting-Edge Grand and Advanced Research (SUGAR) Program, Institute for Extra-Cutting-Edge Science and Technology Avant-Garde Research (X-star). We thank Laurent Zimmerman for technical mentorship and assistance. Christophe Thomazo is thanked for the sampling opportunity. The anonymous reviewers are thanked for their constructive suggestions.

Editor: Maud Boyet

Additional Information

Supplementary Information accompanies this letter at https://www.geochemicalperspectivesletters.org/article2207.

Cite this letter as: Ardoin, L., Broadley, M.W., Almayrac, M., Avice, G., Byrne, D.J., Tarantola, A., Lepland, A., Saito, T., Komiya, T., Shibuya, T., Marty, B. (2022) The end of the isotopic evolution of atmospheric xenon. *Geochem. Persp. Let.* 20, 43–47. https://doi.org/10.7185/geochemlet.2207

References

Almayrac, M.G., Broadley, M.W., Bekaert, D.V., Hofmann, A., Marty, B. (2021) Possible discontinuous evolution of atmospheric xenon suggested by Archean barites. *Chemical Geology* 581, 120405. https://doi.org/10.1016/j.chemgeo.2021.120405

Amelin, Yu. V., Heaman, L.M., Semenov, V.S. (1995) U-Pb geochronology of layered mafic intrusions in the eastern Baltic Shield: Implications for the timing and duration of Paleoproterozoic continental rifting. *Precambrian Research* 75, 31–46. https://doi.org/10.1016/0301-9268(95)00015-W

Avice, G., Marty, B., Burgess, R. (2017) The origin and degassing history of the Earth's atmosphere revealed by Archean xenon. *Nature Communications* 8, 15455. https://doi.org/10.1038/ncomms15455

Avice, G., Marty, B., Burgess, R., Hofmann, A., Philippot, P., Zahnle, K., Zakharov, D. (2018) Evolution of atmospheric xenon and other noble gases inferred from Archean to Paleoproterozoic rocks. *Geochimica et Cosmochimica Acta* 232, 82–100. https://doi.org/10.1016/j.gca.2018.04.018

Bekaert, D.V., Broadley, M.W., Delarue, F., Avice, G., Robert, F., Marty, B. (2018) Archean kerogen as a new tracer of atmospheric evolution: Implications for dating the widespread nature of early life. *Science Advances* 4, eaar2091. https://doi.org/10.1126/sciadv.aar2091

Brasier, A.T., Martin, A.P., Melezhik, V.A., Prave, A.R., Condon, D.J., Fallick, A.E. (2013) Earth's earliest global glaciation? Carbonate geochemistry and geochronology of the Polisarka Sedimentary Formation, Kola Peninsula, Russia. *Precambrian Research* 235, 278–294. https://doi.org/10.1016/j.precamres.2013.06.007

Broadley, M.W., Barry, P.H., Bekaert, D.V., Byrne, D.J., Caracausi, A., Ballentine, C.J., Marty, B. (2020) Identification of chondritic krypton and xenon in Yellowstone gases and the timing of terrestrial volatile accretion. *Proceedings of the National Academy of Sciences* 117, 13997–14004. https://doi.org/10.1073/pnas.2003907117

Farquhar, J., Wing, B.A. (2003) Multiple sulfur isotopes and the evolution of the atmosphere. *Earth and Planetary Science Letters* 213, 1–13. https://doi.org/10.1016/S0012-821X(03)00296-6

Gumsley, A.P., Chamberlain, K.R., Bleeker, W., Söderlund, U., De Kock, M.O., Larsson, E.R., Bekker, A. (2017) Timing and tempo of the Great Oxidation Event. *Proceedings of the National Academy of Sciences* 114, 1811–1816. https://doi.org/10.1073/pnas.1608824114

Hébrard, E., Marty, B. (2014) Coupled noble gas–hydrocarbon evolution of the early Earth atmosphere upon solar UV irradiation. *Earth and Planetary Science Letters* 385, 40–48. https://doi.org/10.1016/j.epsl.2013.10.022

Killingsworth, B.A., Sansjofre, P., Philippot, P., Cartigny, P., Thomazo, C., Lalonde, S.V. (2019) Constraining the rise of oxygen with oxygen isotopes. *Nature Communications* 10, 4924. https://doi.org/10.1038/s41467-019-12883-2

Lyons, T.W., Reinhard, C.T., Planavsky, N.J. (2014) The rise of oxygen in Earth's early ocean and atmosphere. *Nature* 506, 307–315. https://doi.org/10.1038/nature13068

Marty, B., Bekaert, D.V., Broadley, M.W., Jaupart, C. (2019) Geochemical evidence for high volatile fluxes from the mantle at the end of the Archaean. *Nature* 575, 485–488. https://doi.org/10.1038/s41586-019-1745-7

Ozima, M., Podosek, F.A. (2002) *Noble Gas Geochemistry*. Second Edition, Cambridge University Press, Cambridge. https://doi.org/10.1017/CBO9780511545986

Pepin, R.O. (1991) On the origin and early evolution of terrestrial planet atmospheres and meteoritic volatiles. *Icarus* 92, 2–79. https://doi.org/10.1016/0019-1035(91)90036-S

Péron, S., Moreira, M. (2018) Onset of volatile recycling into the mantle determined by xenon anomalies. *Geochemical Perspectives Letters* 9, 21–25. https://doi.org/10.7185/geochemlet.1833

Péron, S., Mukhopadhyay, S., Kurz, M.D., Graham, D.W. (2021) Deep-mantle krypton reveals Earth's early accretion of carbonaceous matter. *Nature* 600, 462–467. https://doi.org/10.1038/s41586-021-04092-z

Philippot, P., Ávila, J.N., Killingsworth, B.A., Tessalina, S., Baton, F., Caquineau, T., Muller, E., Pecoits, E., Cartigny, P., Lalonde, S.V., Ireland, T.R., Thomazo, C., van Kranendonk, M.J., Busigny, V. (2018) Globally asynchronous sulphur isotope signals require re-definition of the Great Oxidation Event. *Nature Communications* 9, 2245. https://doi.org/10.1038/s41467-018-04621-x

Poulton, S.W., Bekker, A., Cumming, V.M., Zerkle, A.L., Canfield, D.E., Johnston, D.T. (2021) A 200-million-year delay in permanent atmospheric oxygenation. *Nature* 592, 232–236. https://doi.org/10.1038/s41586-021-03393-7

Pujol, M., Marty, B., Burgess, R. (2011) Chondritic-like xenon trapped in Archean rocks: A possible signature of the ancient atmosphere. *Earth and Planetary Science Letters* 308, 298–306. https://doi.org/10.1016/j.epsl.2011.05.053

Saito, T., Qiu, H.N., Shibuya, T., Li, Y.B., Kitajima, K., Yamamoto, S., Ueda, H., Komiya, T., Maruyama, S. (2018) Ar–Ar dating for hydrothermal quartz from the 2.4 Ga Ongeluk Formation, South Africa: Implications for seafloor hydrothermal circulation. *Royal Society Open Science* 5, 180260. https://doi.org/10.1098/rsos.180260

Vermeesch, P. (2018) IsoplotR: A free and open toolbox for geochronology. *Geoscience Frontiers* 9, 1479–1493. https://doi.org/10.1016/j.gsf.2018.04.001

Warke, M.R., Di Rocco, T., Zerkle, A.L., Lepland, A., Prave, A.R., Martin, A.P., Ueno, Y., Condon, D.J., Claire, M.W. (2020) The Great Oxidation Event preceded a Paleoproterozoic "snowball Earth". *Proceedings of the National Academy of Sciences* 117, 13314–13320. https://doi.org/10.1073/pnas.2003090117

Zahnle, K.J., Gacesa, M., Catling, D.C. (2019) Strange messenger: A new history of hydrogen on Earth, as told by Xenon. *Geochimica et Cosmochimica Acta* 244, 56–85. https://doi.org/10.1016/j.gca.2018.09.017